# Scaling laws for Beta* in the LHC Interaction Regions

E. Todesco, J.-P. Koutchouk, CERN, Geneva, Switzerland

*Abstract*

A lay-out for the triplet in the low-beta interaction regions of the Large Hadron Collider based on the present baseline is studied. A parametric analysis of the dependence of the beta function in the interaction point and in the triplet on the magnet length and technology (Nb-Ti or $Nb_3Sn$) is carried out. Solutions with large aperture quadrupoles and low beta functions in the interaction point are presented. A final comparison of the triplet lay-outs using different technologies and distance to the interaction point are discussed.

## INTRODUCTION

The Large Hadron Collider (LHC) features two low-beta interaction regions (IR) where triplets of quadrupoles strongly focus the beams to get a beta function $\beta^*$ in the interaction point (IP) of 55 cm [1]. In the present baseline, the geometric luminosity reduction factor due to the crossing angle in the IP prevents from obtaining significantly higher peak luminosities by a reduction of $\beta^*$ below its nominal value [2]. This bottleneck could be bypassed by introducing an early separation dipole D0 in the detectors [3] and/or using crab cavities [4]: in this case, a further reduction of $\beta^*$ would directly increase the peak luminosity. An upgrade relying on the reduction of $\beta^*$ would be easier and faster to implement than a scenario based on the increase of the beam current: for this reason, studies on optics even smaller than 25 cm are ongoing [5].

In this paper we present a parametric analysis based on the approach outlined in [5] and [6] to evaluate the possible options for the triplet lay-out, namely its length, aperture and distance to the IP. Matching the aperture requirements with the gradient-aperture relation induced by the type of superconducting technology, we find a family of solutions for the lay-outs. We point out that large aperture quadrupoles allow reaching $\beta^*$ down to 7 cm. The field quality that can be achieved in large aperture quadrupoles is estimated on the ground of the experience acquired during the LHC and Relativistic Heavy Ion Collider [7] magnet productions [8]. Issues arising from the optics and beam dynamics associated to very large $\beta$ functions in the triplet can be critical: here, we sketch some scaling laws for the geometric aberrations.

We finally show that a comparison of the different options strongly depends on the underlying hypothesis. Results relative to lay-outs with the same triplet length or with the same linear chromaticity are presented.

## BETA FUNCTIONS IN A BASELINE-LIKE TRIPLET LAY-OUT

### *Triplet structure*

We consider a triplet whose structure is similar to the LHC baseline [1], i.e., is made up of two focusing quadrupoles Q1, Q3 of equal length $l_1$, and with two defocusing quadrupoles Q2, each of length $l_2$, in between. Let $l^*$ be the distance of the beginning of the triplet from the IP (see Fig. 1).

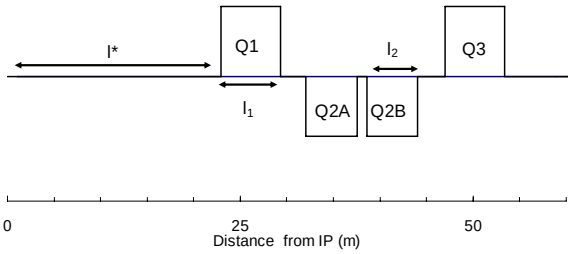


Fig. 1: Nominal lay-out of the triplet close to an LHC IP.

We assume that all the quadrupoles have the same gradient, and we fix the gap between the quadrupoles to the actual values for the nominal LHC baseline (2.7 m between Q1 and Q2A, 1 m between Q2A and Q2B, and 2.9 m between Q2B and Q3). We define $l$ as the average of the length of Q1 and Q2, and $\Delta l$ as the difference

$$l = \frac{l_1 + l_2}{2} \qquad \Delta l = l_1 - l_2; \tag{1}$$

The total length of the quadrupoles and the length of the triplet are defined as

$$l_q = 2(l_1 + l_2) = 4l \qquad l_t = l_q + g \tag{2}$$

where $g$ is the size of the gaps. In the nominal LHC lay-out one has $l^*$=23 m, $l_1$=6.37 m, $l_2$=5.50 m, $l$=5.935 m, $\Delta l$ =0.87 m, $g$=6.6 m, $l_q$=23.74 m and $l_t$=30.34 m.

### *Approximated matching conditions*

We impose the following requirements on the gradient and on the triplet lay-out:

- The triplet must be focusing, i.e. the derivative of the beta functions at the end of Q3 must be negative in both planes.
- One has to avoid a minimum of the beta functions between Q3 and Q4, i.e. the derivative of the beta functions at the entrance of Q4 must be negative in both planes (see Fig. 2).

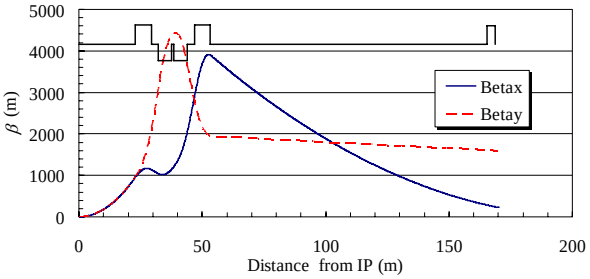


Fig. 2: $\beta$-functions near the IP with nominal LHC lay-out.

For a given triplet structure characterized by $l$, $\Delta l$ and $l^*$, these requirements give a family of solutions parametrized by the quadrupole gradient: we select the gradient that provides the smallest beta functions in Q4, keeping the constraint that they are anyway larger than the beta functions in the regular lattice (i.e. larger than 180 m). The behaviour of the beta functions for the nominal values of the LHC lattice are given in Fig. 2.

### *$\beta$ function and quadrupole gradient vs. lay-out*

We first considered a scenario derived from the nominal one, with $l^*$=23 m, $\beta^*$=55 cm, $l_q$=23.74 m, varying the difference $\Delta l$ between Q1 and Q2 lengths. For each case, we selected the gradient according to the criteria given in the previous section, and we computed the maximum $\beta$ function in the triplet in both planes. One observes that varying $\Delta l$ one can find the optimal condition in which the maximum $\beta$ function is the same in both planes (see Fig. 3). This is not exactly as the nominal case, where the $\beta$ function in one plane is ~10% larger (see Fig. 2).

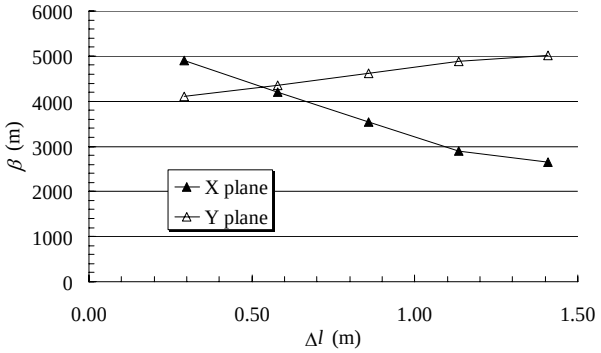


Fig. 3: Maximum $\beta$ function in the triplet versus difference between Q1 and Q2 length for nominal $l$ and $l^*$.

We then vary the total length of the quadrupole $l_q$, and for each case we compute the optimal $\Delta l$ that gives the same maximum $\beta$ function in both planes. Simulations show that for a fixed $l^*$ and $l_q$, the maximum $\beta$ function $\beta_{max}$ is a linear function of the total length of the quadrupoles:

$$\beta_{\max} = A + Bl_q \,. \tag{3}$$

We fix the constant $A$ to the theoretical value for a thin triplet $l^{*2}/\beta^*$, and we explicit the dependence of $B$ on $\beta^*$

$$\beta_{\max} = \frac{l^{*2} + al_q}{\beta^*} \,. \tag{4}$$

The fit of the numerical data with Eq. (4), with $a$ free parameter, is shown in Fig, 4. The value of $a$ versus $l^*$ are given in Table I: $a$ turns out to be proportional to $l^*$:

$$\beta_{\max} \sim \frac{l^*(l^* + el_q)}{\beta^*} \tag{5}$$

with $e$~3.6, within 10%.

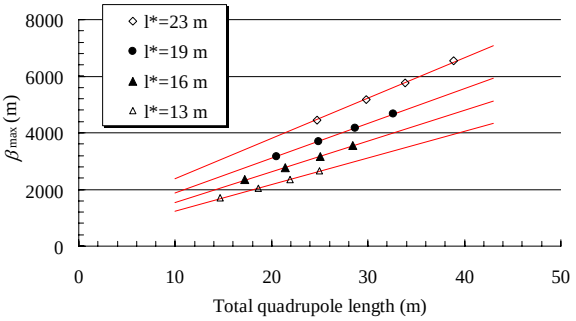


Fig. 4: Maximum $\beta$ in the triplet versus triplet length and distance $l^*$ to the IP.

Table I: Dependence of $a$, as defined in Eq. (4), on the distance to the interaction point

| $l^*$ (m) | $a$ (m) | $e=a/l^*$ (adim) |
|---|---|---|
| 13 | 51.5 | 3.96 |
| 16 | 59.4 | 3.71 |
| 19 | 67.4 | 3.55 |
| 23 | 78.2 | 3.40 |

It must be pointed out that the simple approximation

$$\beta_m \approx \frac{1}{\beta^*}\left(l^* + \frac{l_t}{2}\right)^2 \tag{6}$$

severely underestimates $\beta_m$ for a thick triplet: in the nominal LHC case it gives 2600 m instead of 4500 m.

The same analysis has been carried out for the dependence of the quadrupole gradient $G$ on $l_q$ and $l^*$. The inverse of the gradient is well fit by a second order polynomial in $l_q$ passing though zero (see Fig. 5)

$$G = \frac{1}{fl_q^{\,2} + hl_q} \tag{7}$$

We take a second order polynomial rather than a linear fit since in this way we can impose the physical condition $G$ infinite for zero triplet length (thin lens). The polynomial fit also has the advantage of having $f$ independent of $l^*$ and $h$ proportional to the square root of $l^*$ within 2% in the analyzed range (see Table II), thus giving

$$G = \frac{1}{fl_q^{\,2} + pl_q\sqrt{l^*}} \tag{8}$$

Table II: Dependence of $f$ and $h$, as defined in Eq. (7) of the gradient, on the distance to the interaction point

| $l^*$ (m) | $f$ (1/T) | $h$ (m/T) | $p=c/\sqrt{l^*}$ ($\sqrt{}$m/T) |
|---|---|---|---|
| 13 | 1.90E-06 | 1.07E-04 | 2.96E-05 |
| 16 | 1.90E-06 | 1.25E-04 | 3.12E-05 |
| 19 | 1.90E-06 | 1.38E-04 | 3.17E-05 |
| 23 | 1.90E-06 | 1.55E-04 | 3.22E-05 |

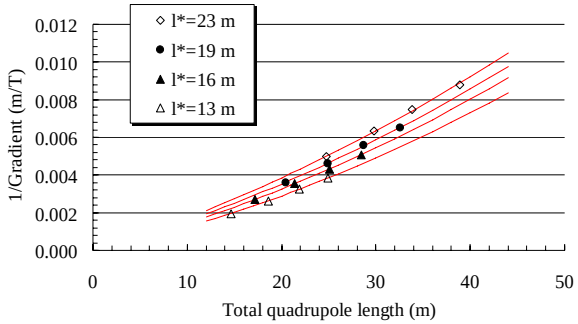


Fig. 5: Inverse of the quadrupole gradient versus triplet length and distance $l^*$ to the IP.

## APERTURE REQUIREMENTS

Here we summarize the standard requirements (see for instance [2,5,6]) for the triplet aperture $\phi$ (diameter) in the LHC, which is given by

$$\phi = \kappa_\beta (d + 2\rho) + 2(A + B + C + D) \tag{9}$$

where $d$ is the separation between the beams, $\rho$ is the radius of the beam, $\kappa_\beta$ the beta beating, and the last four terms are given by alignment tolerances ($A$), beam screen clearance ($B$), closed orbit ($C$), and dispersion ($D$). Please note that in the followings, all equations are for distances given in meters, whereas millimetres will be used in some tables and plots to improving the readability.

The beam radius is taken at 10 sigma

$$\rho = 10\sigma = 10\sqrt{\frac{\varepsilon_n \beta_{\max}}{\gamma}} \tag{10}$$

where $\varepsilon_n$ is the normalized beam emittance ($\varepsilon_n$=3.75 m μrad), and $\gamma$ is the relativistic factor ($\gamma$=7461 at 7 TeV). The beam separation is given by

$$d = 2\theta(l^* + l_t) \tag{11}$$

where $l^*$ and $l_t$ are the distance of the triplet to the IP and its length (2), and $\theta$ is the half crossing angle, that depends on the beam parameters according to the following scaling [9]

$$\theta = \theta_0 \left[ \delta \sqrt{\frac{\beta_0^*}{\beta^*}} + (1-\delta) \sqrt{\frac{\beta_0^*}{\beta^*}} \sqrt{\frac{l^* + l_t}{l_0^* + l_{t0}}} \sqrt{\frac{N_b k_b}{N_{b0} k_{b0}}} \right] \tag{12}$$

where $\theta_0$=142.5 μrad is the nominal half crossing angle, the quantities with the suffix 0 are the nominal ones, and $\delta$=6.5/9.5~0.68. According to this empirical law, around 70% of the crossing angle scales as the inverse of the square root of $\beta^*$ (i.e., a smaller $\beta^*$ gives a larger angle), and the remaining 30% also with the square root of the distance of the end of the triplet from the IP, and with the total number of particles in the machine $N_b k_b$.

The dispersion term $D$ is estimated to be proportional to the maximum $\beta$ function according to

$$D = 0.4\sqrt{\frac{\beta_m}{180}} 0.86 \times 10^{-3}, \tag{13}$$

and the other terms A, B, C are constants, set at 1.6 mm (alignment), 6.6 mm (beam screen) and 3 mm (closed orbit) respectively. The sizes of the different contributions to the quadrupole aperture are given in Table III: the dominant one is the beam size, which accounts for almost half of the aperture, and the beam separation (one fourth). The dispersion and the alignment errors have the smallest contributions (4% each).

Table III: quadrupole aperture budget in the nominal case.

| | (mm) | (%) |
|---|---|---|
| Beam size | 32.7 | 43 |
| Separation | 17.3 | 23 |
| Alignment | 3.2 | 4 |
| Beam screen | 13.2 | 17 |
| Closed orbit | 6.0 | 8 |
| Dispersion | 3.4 | 4 |
| Total | 75.9 | 100 |

The expression (9) for the aperture can be rewritten to explicit the dependence on the beta functions:

$$\phi = \phi_0 + \phi_1 \sqrt{\beta_{\max}} + \phi_2 \frac{l^* + l_t}{\sqrt{\beta^*}} + \phi_3 \frac{(l^* + l_t)^{3/2}}{\sqrt{\beta^*}} \sqrt{N_b k_b} \tag{14}$$

where

$$\phi_0 = 2(A + B + C) \tag{15}$$

$$\phi_1 = 2\left( 10\kappa_\beta \sqrt{\frac{\varepsilon_n}{\gamma}} + 0.4 \frac{0.86}{\sqrt{180}} 10^{-3} \right) \tag{16}$$

$$\phi_2 = 2\kappa_\beta \theta_0 \delta \sqrt{\beta_0^*} \tag{17}$$

$$\phi_3 = 2\kappa_\beta \theta_0 (1-\delta) \sqrt{\frac{\beta_0^*}{(l_0^* + l_{t0}) N_{b0} k_{b0}}}. \tag{18}$$

The values of the coefficients and the relative weight of the different contributions to the aperture budget are given in Table IV. Using the fit given in Eq. (5), we express the aperture as a function of $\beta^*$

$$\phi = \phi_0 + \frac{\phi_4(l^*, l_t, N_b k_b)}{\sqrt{\beta^*}} \tag{19}$$

and the dependence on the triplet lay-out parameters $l^*$ and $l_t$, and on the beam parameters $N_b k_b$ is given by

$$\phi_4 = \phi_1 \sqrt{l^{*2} + e l^* l_q} + \phi_2 (l^* + l_t) + \phi_3 (l^* + l_t)^{3/2} \sqrt{N_b k_b} \tag{20}$$

The parameter $\phi_4$ in the nominal case is ~0.040 $\sqrt{}$m$^3$. The

values of $\phi_4$ for some typical triplet structures and beam parameters are given in Table V. Using the same fit (5) one can also express the aperture as a function of $\beta_m$

$$\phi = \phi_0 + \sqrt{\beta_{\max}}\,\phi_5(l^*, l_t, N_b k_b) \tag{21}$$

where

$$\phi_5 = \frac{\phi_4}{\sqrt{l^*(l^* + el_t)}} \tag{22}$$

and the parameter $\phi_5$ in the nominal case is ~0.00079 √m.

Table IV: Coefficients of Eq. (14) for the quadrupole aperture in the nominal case

| Coefficient | | Contribution | |
|---|---|---|---|
| | | (mm) | (%) |
| $\phi_0$ | 0.022 | 22.4 | 30 |
| $\phi_1$ | 0.00054 | 36.1 | 48 |
| $\phi_2$ | 1.59E-04 | 11.9 | 16 |
| $\phi_3$ | 5.49E-13 | 5.5 | 7 |
| Total | | 75.9 | 100 |

Table V: Dependence of $\Phi_4$ on distance to IP, triplet length, and $N_b k_b$

| $l^*$ | $l_t$ | $N_b k_b$ | |
|---|---|---|---|
| (m) | (m) | Nominal | Nominal*4 |
| 23 | 25 | 0.0404 | 0.0446 |
| 23 | 15 | 0.0330 | 0.0362 |
| 16 | 25 | 0.0333 | 0.0367 |
| 16 | 15 | 0.0266 | 0.0291 |

## GRADIENT VERSUS APERTURE FOR NB-TI AND NB$_3$SN

The maximal gradient that can be obtained for a given aperture depends on the properties of the superconducting material. Here we summarize the results presented in [10]. Nb-Ti is superconducting if the current density $j$ and the magnetic field $B$ are below the critical surface that in the domain of interest can be well fit by

$$j = c(B^*_{c2} - B) \tag{23}$$

with $B^*_{c2}$=13 T at 1.9 K and 10 T at 4.2 K, and $c$=6.00 $10^8$ A/(T m$^2$). The critical gradient, i.e. the gradient obtained when the current density gives a peak field in the coil satisfying Eq. (23), is given by

$$G_c = \frac{B^*_{c2}\kappa c\gamma}{1 + \kappa c\gamma\lambda\dfrac{\phi}{2}} \tag{24}$$

where the filling factor $\kappa$ is the percentage of superconductor present in the insulated cable, and $\phi$ is the magnet aperture (diameter) in meters. The two parameters $\gamma$ and $\lambda$ characterize the coil lay-out, i.e. do not depend on the superconducting properties: $\gamma$ is how much gradient is obtained per unit of current density, and $\lambda$ the ratio between the peak field in the coil and the gradient times the aperture radius. In Ref. [10] it has been shown that for a sector coil of width $w$ one has

$$\gamma = \gamma_0 \log\left(1 + \frac{2w}{\phi}\right) \tag{25}$$

with $\gamma_0$=0.662 $10^{-6}$ Tm/A, and

$$\lambda = a_{-1}\frac{2w}{\phi} + 1 + a_1\frac{\phi}{2w} \tag{26}$$

with $a$=0.1 and $c$=0.06. Substituting (25) and (26) in (24), one obtains

$$G_c = \frac{B^*_{c2}\kappa c\gamma_0 \log\left(1 + \dfrac{2w}{\phi}\right)}{1 + \kappa c\gamma_0\left(a_{-1}\dfrac{2w}{\phi} + 1 + a_1\dfrac{\phi}{2w}\right)\dfrac{\phi}{2}\log\left(1 + \dfrac{2w}{\phi}\right)} \tag{27}$$

The critical gradient as a function of $w$ has a maximum, which is of the order of $\phi$/2. Therefore, for a given aperture $\phi$ and filling factor $\kappa$, one can reach at most the critical gradient

$$G^m_c = \mathrm{Max}_w \frac{B^*_{c2}\kappa c\gamma_0 \log\left(1 + \dfrac{2w}{\phi}\right)}{1 + \kappa c\gamma_0\left(a_{-1}\dfrac{2w}{\phi} + 1 + a_1\dfrac{\phi}{2w}\right)\dfrac{\phi}{2}\log\left(1 + \dfrac{2w}{\phi}\right)} \tag{28}$$

Higher critical gradients can be obtained using $Nb_3Sn$. The critical surface is described through the Kramer law [11], which has the disadvantage of having no explicit solution for the critical gradient. In [10], we proposed an empirical fit in the form

$$j = c\left(\frac{b}{B} - 1\right) \tag{29}$$

with c=4 .00 $10^9$ A/m$^2$ and $b$=23 T at 1.9 K: these values between 11 T and 17 T agree within 5% with the Kramer law using the typical parameters for a very good $Nb_3Sn$ superconductor, namely 3.00 $10^9$ A/m$^2$ at 12 T and 4.2 K. From Eq. (29) one can derive the critical gradient

$$G_c = \frac{\kappa c\gamma}{2}\left(\sqrt{\frac{8b}{\lambda\gamma\phi\kappa c} + 1} - 1\right) \tag{30}$$

and substituting the lay-out parameters (25) and (26) one obtains an explicit expression for the critical gradient in the $Nb_3Sn$ case. As in the Nb-Ti case, the maximum with respect to the coil width $w$ provides the estimate of the higher critical gradient that one can obtain for a given aperture.

In Fig. 6 the values of $G^m_c$ are given for both materials at 1.9 K for a typical 'good' filling factor $\kappa$=0.35. The 80% of the maximum critical gradient is given since an operational margin of 20% is usually applied. The operational values of the LHC MQ (cell quadrupoles) and MQX (triplet quadrupoles) are given. The MQX values are close to the limit of what can be obtained with Nb-Ti. The quench currents reached by the 90 mm aperture

quadrupoles TQS and TQC of the LARP program [12] are also given, together with the 80% of the models developed for the HTQ [13].

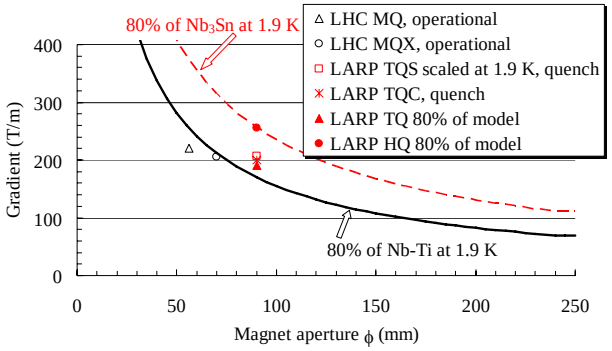


Fig. 6: 80% of the maximal critical gradient versus magnet aperture for Nb-Ti and $Nb_3Sn$ at 1.9 K

$Nb_3Sn$ provides gradients which are around 50% larger for the same aperture with respect to Nb-Ti, but apertures that are 75% larger for the same gradient. This happens since the critical gradient scales with the inverse of the aperture radius only at first order: in Fig. 7 we plot the 80% of the critical gradient times the aperture radius. This quantity is not constant, but varies from 6 T for an aperture of 20 mm up to more than 8 T for apertures larger than 200 mm Therefore, magnets with a large bore are more favorable with respect to the first order scaling. The dependence on the aperture is stronger in the $Nb_3Sn$ case, where the same quantity varies from 8 T (20 mm aperture) to more than 13 T (>200 mm aperture). In the case of 4.2 K instead of 1.9 K, the loss in critical gradient is 23% for the Nb-Ti and 8% for the $Nb_3Sn$.

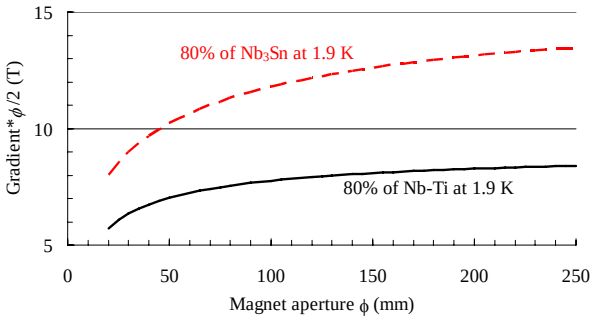


Fig. 7: Maximal critical gradient versus magnet aperture for $Nb_3Sn$ at 1.9 K

## TRIPLET STRUCTURE VERSUS BETA*, SUPERCONDUCTING MATERIAL, AND DISTANCE TO THE IP

We now determine the aperture, gradient and radius of the triplet by intersecting the optics requirements with the superconducting properties. We first fix a distance $l^*$ to the IP; we then consider different $\beta^*$, and different quadrupole lengths $l_q$. For each case, we compute the quadrupole aperture $\phi$ as a function of $l_q$ and $\beta^*$ using Eq. (19), and the gradient $G$ as a function of $l_q$ using Eq. (8). The obtained curves in the space $(G,\phi)$ are shown in Fig. 8: the intersection with the aperture-gradient relation for Nb-Ti and $Nb_3Sn$ quadrupoles given by Eqs. (28) and (30) provides the triplet length, aperture and gradient for a given $\beta^*$.

One finds that for $\beta^*$=55 one can have a Nb-Ti triplet ~25 m long (gap excluded) with 200 T/m and 70mm aperture, which is the present LHC baseline. These are the conditions in which the beam size given by $\beta^*$ and the triplet length match exactly the quadrupole aperture and the gradient compatible with the maximum performances of Nb-Ti. One could obtain a $\beta^*$ of 28 cm with a 30 m long Nb-Ti triplet of 160 T/m and 95 mm aperture, or with a 21 m long $Nb_3Sn$ triplet of 275 T/m and 82 mm aperture. The solutions with Nb-Ti have an aperture of 10%-25% larger than $Nb_3Sn$ (increasing for lower$\beta^*$), and a triplet ~50% longer.

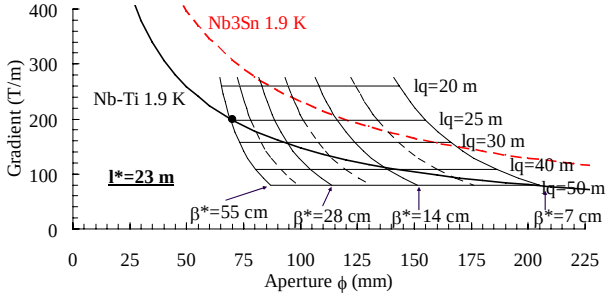


Fig. 8: Quadrupole gradient versus aperture given by Nb-Ti and $Nb_3Sn$ at 1.9 K, and requirements given by $\beta^*$ and total quadrupole length $l_q$ for a distance $l^*$ to the IP of 16 m. Marker: LHC baseline.

In general, one finds that even for very small $\beta^*$, one can build a triplet with the required wide aperture for the beam and with a sufficient integrated gradient to focus it, both for Nb-Ti and $Nb_3Sn$. A shorter distance to the IP allows a smaller aperture (see Figs. 9-11): for $l^*$ =13 m, one can get $\beta^*$ of 28 cm with an aperture of 80 mm and a gradient of 180 T/m in Nb-Ti, or an aperture of 70 mm and a gradient of 300 T/m for the $Nb_3Sn$.

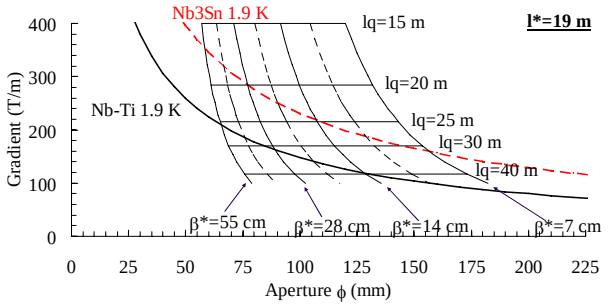


Fig. 9: Quadrupole gradient versus aperture given by Nb-Ti and $Nb_3Sn$ at 1.9 K, and requirements given by $\beta^*$ and quadrupole length $l_q$ for a distance $l^*$ to the IP of 19 m.

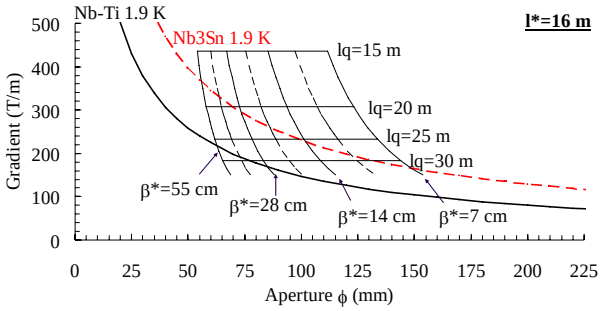


Fig. 10: Quadrupole gradient versus aperture for Nb-Ti and $Nb_3Sn$ at 1.9 K, and requirements given by $\beta^*$ and quadrupole length $l_q$ for a distance $l^*$ to the IP of 16 m.

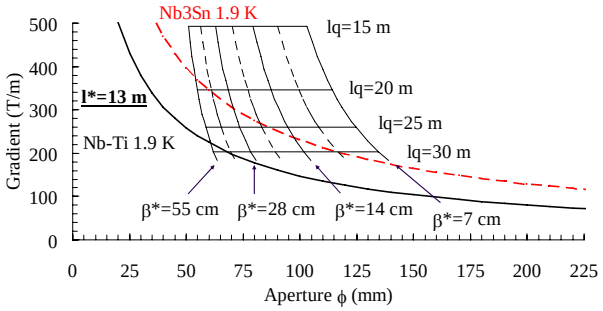


Fig. 11: Quadrupole gradient versus aperture for Nb-Ti and $Nb_3Sn$ at 1.9 K, and requirements given by $\beta^*$ and quadrupole length $l_q$ for a distance $l^*$ to the IP of 13 m.

## LIMITATIONS IN LARGE APERTURE QUADRUPOLES

The results of the previous section show that large aperture quadrupoles allow solutions very a low $\beta^*$. In this section we analyse two possible bottlenecks to having solution with large apertures (i.e. the right parts of Figs. 8-11), namely

- the limitations in the quadrupole due to the stress induced by Lorentz forces, which increases with the aperture
- the field quality that can be reached with a large aperture quadrupole, and the impact on geometric aberrations.

### *Stress due to Lorentz forces*

In this section we review the results given in [13] about the limitations due to the stress induced by the Lorentz forces, which can degrade the cable properties. One can give an analytical estimate of the maximal stress in a 30° sector quadrupole

$$\sigma(r) = \frac{\sqrt{3} j_c^{\,2} \mu_0}{16\pi} \mathrm{Max}_w \frac{1}{r^2}\left[ r^4 - \left(\frac{\phi}{2}\right)^4 + 4r^4 \ln\left(\frac{\phi + 2w}{2r}\right)\right] \tag{31}$$

where $\sigma$ is given in Pa, the maximum has to be taken for $r \in [\phi/2,\ \phi/2+w]$, and $w$ is the coil width. Here, $j_c$ is the critical current whose expression for the Nb-Ti case is

$$j_c = \frac{B_{c2}^* \kappa c}{1 + \kappa c \gamma_0 \log\left(1 + \frac{2w}{\phi}\right)\left(a_{-1}\frac{2w}{\phi} + 1 + a_1 \frac{\phi}{2w}\right)\frac{\phi}{2}} \tag{32}$$

and for the $Nb_3Sn$ is

$$j_c = \frac{\kappa c}{2}\left(\sqrt{\frac{8B_{c2}^*}{\gamma_0 \log\left(1 + \frac{2w}{\phi}\right)\left(a_{-1}\frac{2w}{\phi} + 1 + a_1 \frac{\phi}{2w}\right)\phi \kappa c}} + 1 - 1\right) \tag{33}$$

where the constants used in the equations have been defined in the previous section.

Results for the maximum stress in a Nb-Ti quadrupole as a function of the gradient and of the apertures are given in Fig. 12. Each branch corresponds to the same aperture, and increasing coil widths. Stress increases for larger apertures, but even for the 240 mm case is within 200 MPa, which is a safe value for Nb-Ti: the limit of Nb-Ti is given by insulation rather than by a degradation of the strand due to high pressures.

The case of $Nb_3Sn$ is analyzed in Fig. 13. The maximum tolerable stress is considered to be between 150 and 200 MPa: therefore, quadrupoles with apertures larger than 120 mm can be limited by cable degradation. This problem can be partially solved by reducing the filling factor: for instance, if κ is lowered from 0.35 to 0.25, the stress is reduced by 20%.

The conclusion of this analysis is that quadrupoles with apertures up to 240 mm for Nb-Ti and 120 mm for $Nb_3Sn$ do not suffer from limitations due to the stress induced by Lorentz forces. On the other hand, in $Nb_3Sn$ quadrupoles with very large apertures (more than 120 mm) the stress should be carefully analysed and strategies should be used to avoid reaching the damage limit of the material.

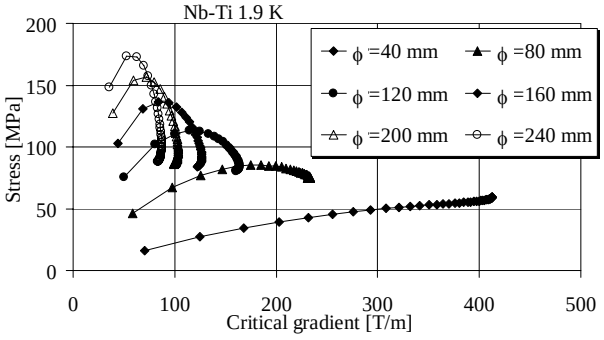


Fig. 12: Maximum stress versus critical gradient for different quadrupole apertures, for Nb-Ti at 1.9 K, with filling factor κ=0.35.

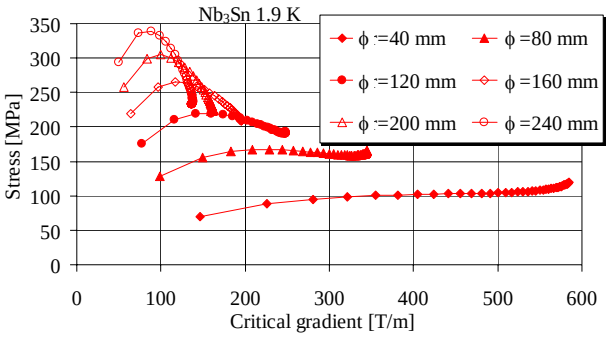


Fig. 13: Maximum stress versus critical gradient for different quadrupole aperture, with Nb-Ti at 1.9 K, and filling factor κ=0.35

## *Field quality*

In this section we summarize the results of the analysis carried out in [8] on the dependence of the field distortions on the magnet inner bore diameter. The quality of the magnetic field is defined through the multipolar expansion

$$B_y + iB_x = 10^{-4} B_2 \sum_{n=2} (b_n + ia_n)\left(\frac{x+iy}{R_{ref}}\right)^{n-1} \qquad (34)$$

where $b_2$=$10^4$ refers to the main component of the quadrupole, and the reference radius $R_{ref}$ is usually taken as 1/3 of the magnet aperture $\phi$. A coil lay-out respecting the quadrupole symmetry has zero multipolar coefficients except $b_{4n+2}$, called the 'allowed' components. Due to tolerances on components and assembly procedures, the symmetry is broken and non-zero multipoles of all orders are generated.

For a given set of magnets, one can define the systematic (average) and the random (standard deviation) components of the field harmonics. The systematic components of the allowed multipoles are a property of the coil cross-section and can be set on any value by an appropriate design of the blocks. The systematic of the non-allowed components are zero in absence of systematic asymmetries of components or procedures. In case of an ideal design setting all systematic multipoles to zero, the random components determine the field quality that can be obtained in a single magnet, and the precision that can be reached for setting the systematic to zero for a finite, small number of magnets (a few units in our case). Therefore, the estimation of the random components in a given coil lay-out is the key ingredient to have an estimate of the expected field quality.

When superconducting quadrupoles are powered to the operational condition at collision energy, the random components of the field harmonics are dominated by the geometric part, i.e. the precision in the positioning of the conductors. In fact, the contribution to the random part of the iron saturation and deformation due to Lorentz forces is negligible. Using a numerical code, one can generate several coil lay-outs whose cable blocks are randomly displaced around the nominal values, and evaluate the induced random components in the field harmonics. One finds that they roughly obey the simple scaling

$$\sigma(b_n) \sim \sigma(a_n) \sim dA\left(\frac{2R_{ref}}{\phi}\right)^n \qquad (35)$$

where $d$ is the standard deviation of the position of the coil blocks, and $A$ is a constant depending on the coil lay-out. Having the standard deviation of the field harmonics relative to a magnet production, and the constant $A$ for that coil lay-out, one can determine the $d$ that better fits the measurements. Results relative to RHIC [7] and LHC production [1] are given in Fig. 14: $d$ ranges from 0.01 mm to 0.03 mm.

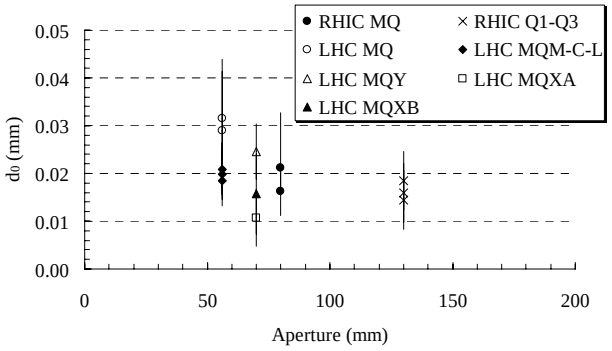


Fig. 14: Coil positioning $d$ versus aperture derived from magnetic measurement of seven types of superconducting quadrupole.

One can prove that that a magnification of the coil lay-out (see Fig. 15), together with a magnification of the precision of positioning, leads to the same random harmonics

$$\sigma(b_n, a_n; \alpha\phi, \alpha d) = \sigma(b_n, a_n; \phi, d) \qquad (36)$$

if the reference radius is always defined as 2/3 of the aperture radius.

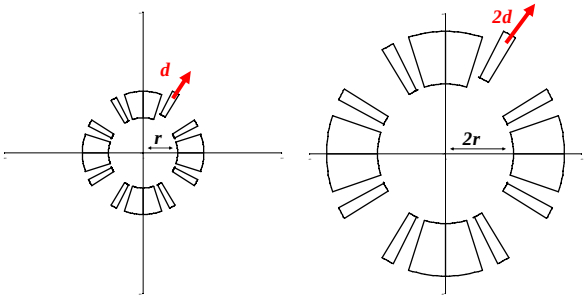


Fig. 15: Magnification of coil lay-out and of coil misplacement leading to the same multipolar components.

From Table IV there is no evidence that a magnet with larger aperture has a larger random displacement $d$. In the RHIC case a 50% increase in the magnet aperture gives a 20% increase of $d$, with very similar coil lay-outs. In the LHC case, the 15% difference in aperture between MQ, MQM and MQY MQX does not reflect in a larger $d$. It is probably more justified assuming $d$ as independent of the magnet aperture and therefore one finds

$$\sigma(b_n, a_n; \alpha\phi, d) = \frac{1}{\alpha}\sigma(b_n, a_n; \phi, d) \quad (37)$$

i.e. that the random components of the field harmonics scale with the inverse of the aperture.

### *Geometric aberrations*

We now consider the effect of the estimated field quality on the beam dynamics. We begin by analyzing the first order amplitude-dependent tuneshift induced by the octupolar term $b_4$ of an IR quadrupole, which is proportional to

$$\Delta Q \propto \int K_3 \beta^2 ds \quad (38)$$

where $K_3$ is defined as

$$K_3 \equiv \frac{1}{B\rho}\frac{\partial^3 B_y}{\partial x^3} = \frac{B_2}{B\rho}\frac{b_4}{R_{ref}{}^3} = \frac{G}{B\rho}\frac{b_4}{R_{ref}{}^2} \quad (39)$$

and $G=B_2/R_{\rm ref}$ is the nominal field gradient in T/m. If we increase the aperture by a factor $\alpha$

$$\phi \to \alpha\phi\,, \quad (40)$$

and the reference radius

$$R_{ref} \to \alpha R_{ref}\,, \quad (41)$$

according to the results of the previous section, the multipoles rescale according to

$$b_4 \to \frac{b_4}{\alpha}\,. \quad (42)$$

The aperture $\phi$ required in a low-β quadrupole is given by

$$\phi = \phi_0 + \phi_5\sqrt{\beta_{\max}}\,; \quad (43)$$

where $\beta_{\max}$ is the maximum beta function quadrupole, and $\phi_0$ and $\phi_5$ are the constants defined in (15) and (22). We now consider two alternative scenarios.

Scenario 1: we assume that a larger aperture of the low-$\beta$ quadrupole is used to house a larger beam and not, for instance, to have an additional shielding; in this case one has

$$\beta \to \left(\frac{\alpha\phi - \phi_0}{\phi - \phi_0}\right)^2 \beta = \alpha^2\left(\frac{\alpha\phi - \phi_0}{\alpha\phi - \alpha\phi_0}\right)^2 \beta \equiv \alpha^2\eta^2\beta \quad (44)$$

For instance in the nominal lay-out of the LHC, one has $\phi$=70 mm and $\phi_0$=22 mm, thus giving $\eta$=1.2 for doubling the aperture $\alpha$=2. One can consider the integrated gradient as a constant,

$$\int G ds \to \int G ds \quad (45)$$

and therefore the integrated multipole scales with

$$\int K_3 ds \to \alpha^{-3}\int K_3 ds \quad (46)$$

and

$$\Delta Q \to \eta^4\alpha\Delta Q \quad (47)$$

i.e. a double aperture quadrupole used to increase of a factor 6 the $\beta$ function leads to an increase in the detuning of a factor 4.

Scenario 2: we assume that the low-β quadrupole aperture is increased to have an additional shielding (i.e., increasing $A$ in Eq. 13) but keeping the same beam size, one has

$$\beta \to \beta \quad (48)$$

and therefore the scaling is

$$\Delta Q \to \alpha^{-3}\Delta Q\,. \quad (49)$$

In the case $\alpha$=2 (doubling the aperture of the triplet from 70 mm to 140 mm), one obtains an increase of the detuning with amplitude of a factor 4 in the first case, and a decrease of a factor 8 in the second one.

These results can be generalized to higher order (see [8] for more details). In general, if the first scenario is considered, the geometric aberrations tend to increase at least linearly with the quadrupole aperture. Therefore, a numerical evaluation of the impact of large aperture quadrupoles on beam dynamics should be carried out [14]. On the other hand, if the additional quadrupole aperture is not used for a larger beam size, the nonlinear contributions are reduced by a factor which is inversely proportional to the aperture increase to the power of the multipole order.

## COMPARISON OF DIFFERENT OPTIONS

### *Criteria for the comparison*

We shown that in principle a very low $\beta^*$ can be obtained in the IP with triplets made of either Nb-Ti or $Nb_3Sn$, in case of no constraints on the available space. Moreover, optics lay-out with large apertures quadrupoles should not be drastically limited by geometric aberrations or by the stress due to Lorentz forces. However, it must be pointed out that any comparison between different triplet lay-outs strongly depends on the selected criteria, which determine different cuts of the parameter space shown in Figs. 8-11, and may lead to different results.

For instance, the analysis of Fig. 8 shows that if we fix the quadrupole length at 25 m, Nb-Ti can provide a $\beta^*$ of 55 cm, but with $Nb_3Sn$ one can arrive up to 14 cm, i.e., one gains a factor 4 in $1/\beta^*$. One the other hand, if we fix the quadrupole aperture to 95 mm, with Nb-Ti we have $\beta^*$=28 cm and with $Nb_3Sn$ we can reach a $\beta^*$ of 20 cm, i.e. we gain only 40% in $1/\beta^*$. The same happens if we want to estimate the gain in reducing the distance to the IP $l^*$.

Here we will carry out the analysis by applying two different criteria: a fixed length of the triplet, imposed by the hardware cost or by the tunnel geometry, or a fixed amount of linear chromaticity, imposed by the correctors. In both cases we estimated the gain in $1/\beta^*$ due to the superconducting technology and to a reduced distance to the IP.

### *First criteria: triplet length*

We consider the nominal case with a distance to the IP of 23 m, and we evaluate which $\beta^*$ can be reached with a triplet length ranging from 20 m to 40 m. A longer triplet requires a lower field gradient in the transverse cross-section, thus allowing wider apertures and a smaller $\beta^*$.

An increase of the triplet length from 25 to 30 m already allows a gain of a factor 2 in $\beta^*$, keeping the same Nb-Ti technology (see Fig. 16); the gain increases to a factor 4 for a triplet of 40 m. $Nb_3Sn$ provides for the same nominal length of 25 m a gain of more than a factor 4 with respect to Nb-Ti, and a factor 7 for a triplet length of 30 m.

The factor 4 can be easily understood: for a fixed triplet length, $Nb_3Sn$ allows an increase of the magnet aperture of ~75% (see Fig. 8), i.e. from 70 mm to 120 mm. This means that the space for the beam increases from 48 mm to 98 mm ($\phi_0$=22 mm, see Eq. 15, 19 and Table IV), i.e. it doubles. Since the beta function is proportional to the square of the beam size, the gain is a factor 4.

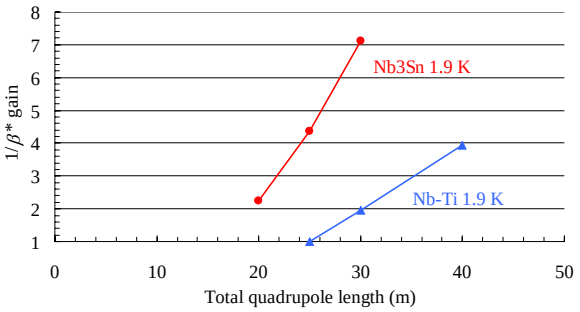


Fig. 16: Gain in $1/\beta^*$ with respect to nominal situation for Nb-Ti and $Nb_3Sn$ fixing the triplet lengths, for $l^*$=23 m.

### *Second criteria: linear chromaticity*

The second comparison is done by setting the linear chromaticity

$$Q' = \int \frac{G}{B\rho}\beta ds \qquad (50)$$

to the same value of the baseline. If the $Nb_3Sn$ is used, this allows for the same $\beta^*$ to have higher gradients, i.e. a more compact triplet; this gives a lower $\beta_m$ and a lower $Q$'. The value of $\beta^*$ can therefore be reduced until when the linear chromaticity recovers the previous value of the baseline. In this way one can estimate the gain in $1/\beta^*$ due to $Nb_3Sn$. In a similar way one can estimate the gain due to a reduction of the distance $l^*$ to the IP. Results are shown in Fig. 17: for a nominal $l^*$, the gain due to $Nb_3Sn$ is 23%. Both Nb-Ti and $Nb_3Sn$ solutions present a gain of up to 20% when $l^*$ is reduced to 13 m. For a $Nb_3Sn$ triplet at 13 m the gain with respect to the nominal lay-out is around 50%. All the solutions shown in Fig. 17 have the same linear chromaticity of the present baseline. It should be noted that the arc sextupole can correct a larger chromaticity, allowing further gains.

A simplified estimate to better understand this result can be carried out: the chromaticity is assumed to be proportional to $\beta_{max}$ times the integrated gradient:

$$Q' = \int \frac{G}{B\rho}\beta ds \propto \beta_{max}\int G ds \qquad (51)$$

and if we keep the same aperture, the material provides an improvement in the gradient of a factor α

$$\hat{G} = \alpha G\,. \qquad (52)$$

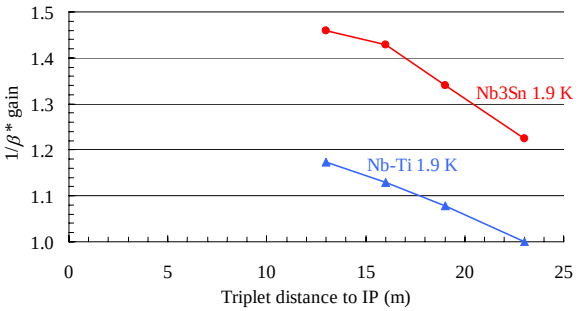


Fig. 17: Gain in $1/\beta^*$ with respect to nominal situation for Nb-Ti and $Nb_3Sn$ and different distances $l^*$ to the IP, having fixed the chromaticity.

where the quantities with the hat denote the $Nb_3Sn$ solution. Assuming that the integrated gradient is constant, the condition on constant chromaticity becomes a condition on equal $\beta_{max}$

$$\hat{\beta}_{max} = \beta_{max} \qquad (53)$$

And using equation (5) one obtains

$$\frac{l^{*2} + a\hat{l}_q}{\hat{\beta}^*} = \frac{l^{*2} + a l_q}{\beta^*}\,, \qquad (54)$$

thus giving

$$\frac{\beta^*}{\hat{\beta}^*} = \frac{l^{*2} + a l_q}{l^{*2} + a\hat{l}_q}\,; \qquad (55)$$

assuming that the aperture is constant, the triplet length is reduced by a factor α

$$\hat{l}_q = \frac{l_q}{\alpha} \qquad (56)$$

and therefore one has

$$\frac{\beta^*}{\hat{\beta}^*} = \frac{l^{*2} + a l_q}{l^{*2} + \frac{a l_q}{\alpha}} = \alpha\frac{l^{*2} + a l_q}{\alpha l^{*2} + a l_q} \equiv \alpha\chi \qquad (57)$$

One can show that $\chi$<1, i.e. the gain α due to the material is only partially transferred to $1/\beta^*$. For the nominal case $l^*$=23 m, $l_q$=24 m, $a$=80 m; if we now switch to $Nb_3Sn$, we have an approximate 50% gain α=1.5, but $\chi$=0.90 and then $\alpha\chi$=1.35, i.e. the gain in $1/\beta^*$ is 35% (see Fig. 18).

If the exact computation is carried out, i.e. taking into account the difference in apertures between the materials induced by the optics (10% between $Nb_3Sn$ and Nb-Ti), and that the condition of the integrated gradient is not exactly satisfied so that $l_q$ is not simply inverse proportional to $G$, one obtains the results shown in Fig. 17, i.e. $Nb_3Sn$ provides 22% more than Nb-Ti. Since the intercept of $\beta_{max}(l_t)$ is proportional to $l^*$ (see Eq. 5), only in the case $l^*$=0 the gain in $\beta_{max}$, i.e., in $1/\beta^*$, is equal the gain in gradient induced by the technology.

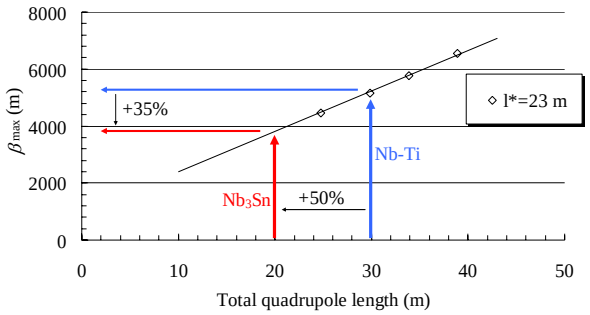


Fig. 18: Simplified plot showing the reduction of $\beta_{max}$ induced by using a triplet of $Nb_3Sn$ instead of Nb-Ti.

## CONCLUSIONS

In this paper we studied a triplet based on the LHC lay-out, made up of three quadrupoles Q1-Q3 with the same gradient and aperture, and with two different lengths Q2 and Q1=Q3. Using a semi-analytical approach, we gave a parametric dependence of the maximum of the beta function and of the quadrupole gradient on the distance to the IP $l^*$, on the beta function in the IP $\beta^*$, and on the total length of the quadrupoles $l_q$, [see Eqs (5) and (8)]. These equations allowed to study a three-parameter family of solutions for the IR optics, including the aperture requirements in each case. We varied $\beta^*$ from 55 to 7 cm.

We then recalled the results of [10] relative to the maximum gradient that can be achieved for a given aperture using Nb-Ti or $Nb_3Sn$ technology [see Eq. (28) and (30)]. The intersection of the optics solutions with the technology constraints (Figs. 8-11) showed that in principle both Nb-Ti and $Nb_3Sn$ allow reaching a $\beta^*$ of 7 cm with this triplet lay-out (cases with lower $\beta^*$ were not considered), with apertures as large as 200 mm.

This result led us to investigate if there are some limitations to lay-outs with large aperture quadrupoles. We first analysed the problems related to the stress induced by the Lorentz forces in such powerful, large magnets. We recalled a scaling law [13] showing that for the Nb-Ti the stress is not an issue, but that for $Nb_3Sn$ apertures larger than 120 mm could have a stress limiting the superconductor performances. Then, we estimated the impact of the expected field quality and of large beta functions in the triplet on the beam dynamics. Large aperture quadrupoles are shown to have a better field quality (see Eq. 37), but if the larger aperture is used to house a larger beam, the geometric aberrations can become critical, requiring adequate correction schemes.

Finally, we compared the different lay-outs to estimate the gain in $1/\beta^*$. We pointed out that the results strongly depend on the criteria used for the comparison. If the length of the triplet is the hard constraint, the gain obtained by using $Nb_3Sn$ instead of Nb-Ti is more than a factor 4. On the other hand, if the limitation is due to the correction of the linear chromaticity, the gain of $Nb_3Sn$ technology is only 20-30%, and reducing the distance of the triplet to the IP to 13 m one obtains an additional gain around 20-25%.

Ignoring the power deposition issue, the gain due to $Nb_3Sn$ technology varies in a large range (from 20% to a factor 4) depending on the imposed constraints. For very high luminosities, the power deposition temperature margin and the heat extraction issues may become determinant for the technology choice. They require dedicated studies, which are in progress.

## REFERENCES

[1] AA. VV. "LHC Design Report", CERN **2004-003** (2004).
[2] O. Bruning, et.al., "LHC Luminosity and energy upgrade: a feasibility study", LHC Project Report **626** (2002).
[3] G, Sterbini, J.P. Koutchouk, these proceedgins.
[4] R. Calaga, there proceedings.
[5] J.P. Koutchouk, "Investigations of the Parameter Space for the LHC Luminosity Upgrade", LHC Project Report **973** (2006).
[6] J.P. Koutchouk, these proceedings.
[7] M. Anerella et al., "The RHIC magnet system", *Nucl. Instrum. Meth.* **A499** (2003) 280-315.
[8] B. Bellesia, J.P. Koutchouk, E. Todesco, in preparation.
[9] F. Zimmermann, private communication.
[10] L. Rossi, E. Todesco, "Electromegnetic design of superconducting quadrupoles", *Phys. Rev. STAB* **9** (2006) 102401.
[11] E. J. Kramer, "Scaling laws for flux pinning in hard superconductors", *J. Appl. Phys.* Vol. 44, pp. 1360-70, 1973.
[12] S. Gourlay et al., "Magnet R&D for the US LHC Accelerator Research Program (LARP)", *IEEE Trans. Appl. Supercond.* **16** (2006) 324-7.
[13] P. Fessia, F. Regis, E. Todesco, "Parametric analysis of forces and stresses in superconducting quadrupole sector windings", ASC06, IEEE Trans. Appl Supercond., in press.
[14] R. De Maria, O. Brüning, these proceedings.